

THE 4TH INTERNATIONAL CONFERENCE ON ALUMINUM ALLOYS

THE EVOLUTION OF NUCLEATION SITES FOR CUBE RECRYSTALLISATION TEXTURE DURING HOT DEFORMATION OF ALUMINIUM

H.E. Vatne¹, R.K. Bolingbroke² and E. Nes¹

1. The Norwegian Institute of Technology, Department of Metallurgy,
N-7034 Trondheim, Norway

2. Alcan International Limited, Southam Road, Banbury, Oxon, England

Abstract

Plain strain compression of an AA1050 aluminium alloy has been used to follow the evolution of nucleation sites for the cube recrystallisation texture component. Specimens were hot deformed to strains in the range $\epsilon=0.5$ to $\epsilon=2$ at various strain rates and temperatures. The cube oriented grains that were present in the material prior to deformation, remained metastable during the deformation process. By studying cube-oriented areas with the EBSP-technique, it was found that their relative stability depends on both strain and Zener-Hollomon parameter. The volume fraction of cube decreased with both increasing strain and Zener-Hollomon parameter. The stable cubes were observed to deform to elliptically shaped grains which upon continued straining were smeared out to long bands. The interior of the bands were of cube orientation while the periphery often contained large misorientations. The cube bands have a unique subgrain size distribution with larger subgrains than other texture components. This makes the cube bands very potent nucleation sites. The probability of nucleation from the cube bands have been found to depend on the orientation of the neighbour components surrounding the band.

Introduction

The cube orientation is often found to be the strongest recrystallisation texture component after annealing of hot deformed aluminium. Since cube is of great technological relevance much effort has been put into explaining its origin. The strong cube recrystallisation texture has been explained both through theories of oriented nucleation [1] and oriented growth [2]. While the Dillamore-Kato mechanism [3] predicts the rotation of ND-rotated cube grains into the metastable cube orientation during deformation, others [4] assume that old cube oriented grains remain metastable during deformation. These pre-existing cube oriented areas will, upon annealing, act as nucleation sites for the cube recrystallisation texture.

Duggan et al. [5] and Vatne et al. [6] investigated nucleation from cube bands (assumably old cube grains being smeared out to band-like features during deformation) in copper and aluminium, respectively. They found that the probability of nucleation from cube bands was enhanced when the bands were surrounded by the $S=\{123\}<634>$ deformation texture component.

This preference can be attributed to either a micro-growth selection, due to a higher mobility of the $40^\circ\langle 111 \rangle$ oriented cube-S tilt boundary, or preferred nucleation, due to the lower energy of the cube-S $\Sigma 7$ boundary, resulting in a smaller critical Gibbs-Thomson radius requirement. The special orientation topography between a cube band and an S oriented grain might be more prone to collapse into a high angle boundary than others. Finally, the amount of stored energy may be higher in the S deformation texture component (for a detailed discussion, see [6,7]).

In the present work, the stability of cube oriented areas during deformation of an AA1050 alloy has been investigated. After deformation at different conditions, all cube areas were characterised with respect to size and subgrain sizes. An eventual neighbour preference of nucleation from cube oriented areas surrounded by S has been examined, both on a micro level utilizing the EBSP-technique and on a macro level by X-ray measurements.

Experimental

All experiments were carried out on an AA1050 commercial purity aluminium alloy with chemical composition Al-0.3%Fe-0.1%Si (wt%). In order to have a controlled set of deformation conditions, specimens were plain strain compressed at Alcan International, Banbury Laboratory. For investigations of cube stability during deformation, material with a volume fraction of 10% cube and an average grain size of $47\mu\text{m}$ was chosen. Specimens were deformed to strains in the range $\epsilon=0.5$ to $\epsilon=2$ and Zener-Hollomon parameters ($Z=\dot{\epsilon}\exp[Q/RT]$) $Z=6.7\cdot 10^{12}$ ($\dot{\epsilon}=2.5$, 400°C) to $Z=9.8\cdot 10^{15}$ ($\dot{\epsilon}=25$, 300°C). For convenience, the material for subgrain size measurements and S/cube neighbour preference investigations was processed in a way as to achieve a starting material with about 25% cube and 20% S. This material was plain strain compressed to a strain of $\epsilon=2$ and a Zener-Hollomon parameter $Z=10^{14}$ ($\dot{\epsilon}=0.6$, 300°C), water-quenched and subsequently annealed at 300°C .

Macroscopic texture was measured by an automatic X-ray diffractometer. ODFs were produced from four incomplete pole figures ($\{111\}$, $\{200\}$, $\{220\}$, $\{113\}$) by the series expansion method [8]. All micro-structure/texture investigations were carried out by means of the SINTEF EBSP-system attached to a Jeol 6400 scanning electron microscope. The system allows for a rapid, accurate and simple on-line orientation determination of single subgrains larger than $\sim 0.5\mu\text{m}$. An accuracy of $\sim 1^\circ$ in the orientation determination is obtained.

EBSP-scans were made in the longitudinal-transverse section. Cube areas in this section were typically of a band-like shape with a length/width ratio depending on deformation conditions. To investigate the stability of cube oriented areas during deformation, the width of cube bands were measured for various degrees of deformation. The EBSP-technique was also utilised to measure subgrain sizes within and outside cube bands. The EBSP-technique gives a much more reliable result than measurements on SEM-micrographs. All subgrain sizes were measured in the deformation direction.

An important part of the present work was to reproduce, both macro- and microscopically, the importance of the S deformation texture component for the dominance of the cube recrystallisation texture. Therefore, a set of materials with variations in the contents of initial S and cube was processed and the strength of cube in the recrystallised condition determined by X-ray measurements. One of these conditions (the one with 25% cube and 20% S) was chosen for further microscopic characterisation of the cube bands and their neighbours. The orientation

of the band itself and the orientations of the adjacent neighbouring components were determined by means of EBSP. This was carried out in the as deformed and several partly recrystallised conditions (for different fractions of recrystallisation, cf. Table 2). Since a successful nucleation event destroys the information about the nucleus state itself as well as the original neighbours, transformed bands were not taken into consideration. Only those bands where no nucleation had taken place (untransformed bands) were investigated for orientation relationships.

Results

Figure 1 shows the results of the investigations of the cube stability during deformation. The figure is based on EBSP-scans in the normal direction in the transverse-longitudinal section. In Fig. 1a) the average width of all detected cube areas is shown, b) shows the band width distribution while the line fraction of cube is shown in c). Both the width and the line fraction is plotted as a function of strain for different Zener-Hollomon parameters. In the starting material a line fraction of about 16% of cube is found. This value differs from the volume fraction found to be about 10% by X-rays. This discrepancy is, however, not surprising, since the two methods are very different and uncertain. In both cases a deviation of 15° off the ideal cube orientation was accepted. An EBSP-scan analysis will, however, overestimate the fraction of cube, since subgrains within a cube band with rotations slightly greater than 15° off cube have been assumed to belong to the cube band. Therefore, the line fractions should not be taken as absolute values, but be used for comparison between the different deformation conditions. Figure 1 shows that the fraction of cube decreases with increasing strain. This is also demonstrated by macro texture measurements for 1050 material ($Z=6.7 \cdot 10^{12}$, $\xi=2.5$, 400°C) of various initial cube fractions in Fig. 1d). Also, the band widths decrease with increasing strain, roughly in accordance with what is expected for a pure compression of the original cube oriented grains in the starting material (dotted line in Fig. 1a)). The plot in b) shows how the distribution of cube band widths gradually gets narrower with increasing strain, starting from a broad specter of the initial cube grains present in the material prior to the deformation (denoted $\epsilon=0$).

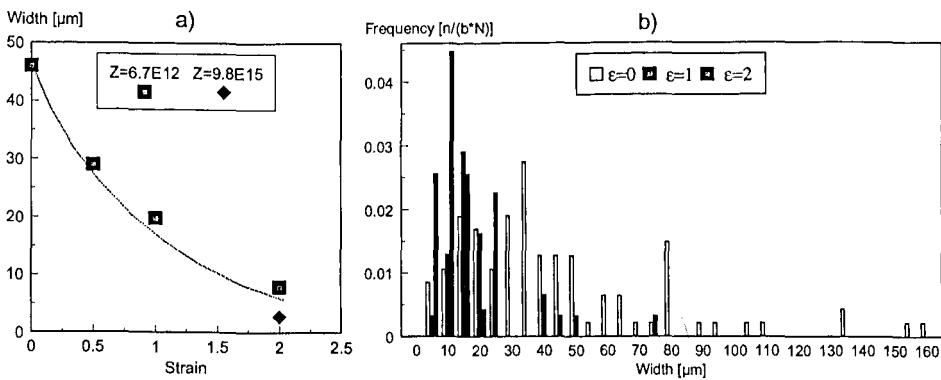


Figure 1. a) average cube band width, b) distribution of band widths ($Z=6.7 \cdot 10^{12}$, $\xi=2.5$, 400°C)

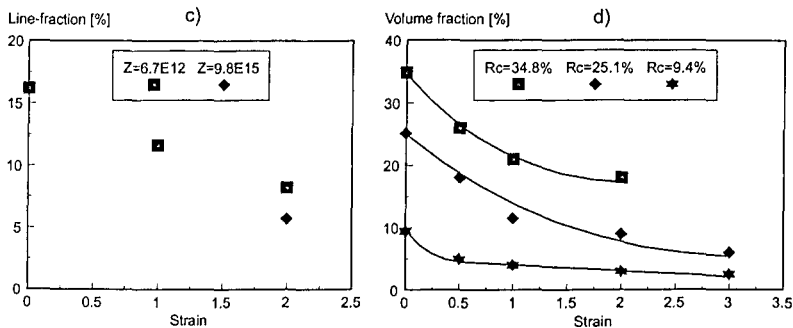


Figure 1. c) Line fraction of cube, EBSP, d) Volume fraction of cube, X-ray ($Z=6.7 \cdot 10^{12}$, R_c =initial cube fraction)

In Fig. 2 the subgrain size distribution of the as deformed (and quenched, $\epsilon=2$, $Z=10^{14}$) condition for cube oriented subgrains within cube bands (a) compared to subgrains of other orientations (b) is plotted. Both show an approximately log-normal distribution. However, the cube subgrain size distribution shows a longer tail of large subgrains which is not found for other orientations. It should be noted that these large subgrains are in fact overcritical nuclei being present in the cube bands already in the as deformed state. Due to the longer tail the cube subgrains are on average larger than the other subgrains, $3.8\mu\text{m}$ vs. $2.9\mu\text{m}$, respectively. After 2h of annealing ($\sim 25\%$ recrystallised) the average subgrain sizes have increased to $5.1\mu\text{m}$ (cube) and $4.6\mu\text{m}$ (others), Table 1. Only real subgrains and no recrystallised grains have been considered. The size difference is no longer so pronounced in the partially recrystallised condition, which is most likely due to that the largest cube subgrains have been transformed into recrystallised grains.

Table 1: Average subgrain size, $\epsilon=2$, $Z=10^{14}$ ($\xi=0.6$, 300°C), annealed at 300°C

% recrystallised	0% (as deformed)	25% (2h annealed)
Cube	$3.8\mu\text{m}$	$5.1\mu\text{m}$
Others	$2.9\mu\text{m}$	$4.6\mu\text{m}$

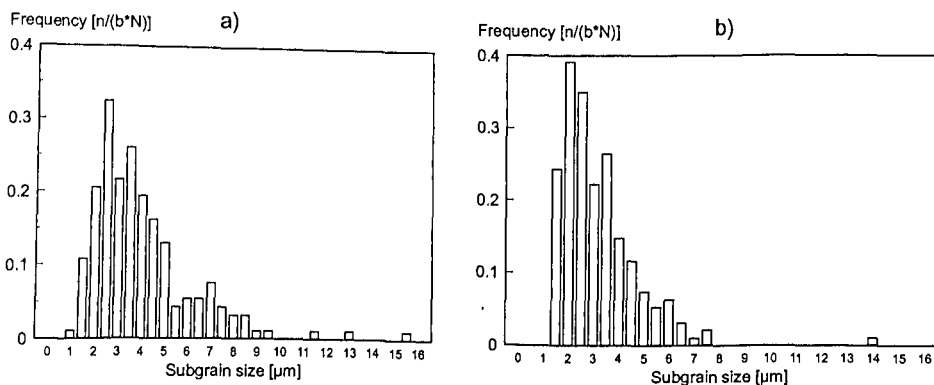


Figure 2. Subgrain size distributions: a) cube, b) others, $\epsilon=2$, $Z=10^{14}$ ($\xi=0.6$, 300°C)

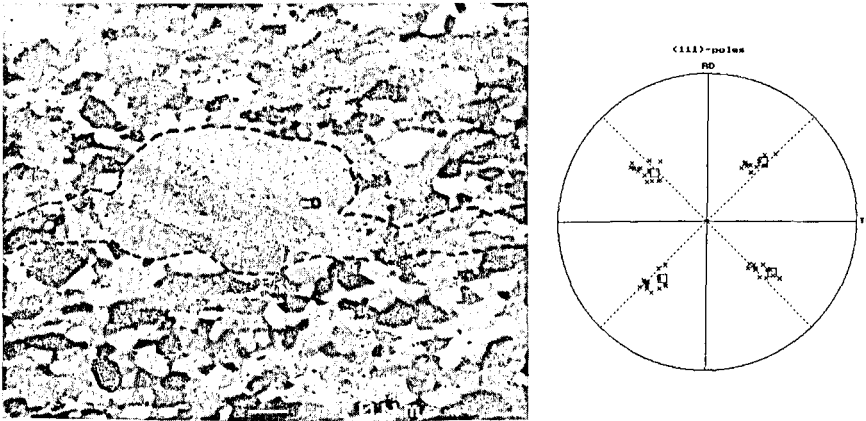


Figure 3. SEM micrograph of nucleation from cube band, \square =recrystallised cube grain, x =subgrains within cube band

A SEM micrograph of the nucleation event from a cube band is shown in Fig. 3. The importance of the orientation of the neighbour component adjacent to the cube band is demonstrated in Fig. 4. Only boundaries between S and cube bands were analysed, since these $40^\circ\langle 111 \rangle$ boundaries of assumably high mobility and low energy have been found to promote nucleation from cube bands [5,6]. In Fig. 4a) the fraction of untransformed cube bands (i.e. bands where no nucleation event has taken place) surrounded by a $40^\circ\langle 111 \rangle$ boundary is plotted. For a boundary to be characterised as a $40^\circ\langle 111 \rangle$ type, deviations of maximum $\Psi_{\max}=10^\circ$ from an ideal $\langle 111 \rangle$ rotation axis and $\Phi_{\max}=15^\circ$ from an ideal 40° rotation angle were accepted. These limits were chosen based on the elegant observations by Liebmann-Lücke-Masing [9] who found that the growth advantage of $40^\circ\langle 111 \rangle$ boundaries falls off significantly when these limits are reached. In the as deformed condition about 20% of the cube bands were surrounded by $40^\circ\langle 111 \rangle$. Throughout the transformation this fraction decreased considerably (down to 9%). Statistically, this means that most of the bands which were originally surrounded by $\Sigma 7$ -type boundaries have been transformed, i.e. a successful nucleation and subsequent growth has taken place. On the other hand, cube bands which were not surrounded by such boundaries did not show the same ability to provide recrystallised cube grains. Detailed data of this experiment is given in Table 2. A similar trend has previously been reported by Vatne et al. [6] by performing a similar experiment with a hot rolled 3004 alloy. The results of this investigation is also included in Fig. 4.

Table 2: Results from the EBSD-analysis of untransformed cube bands followed throughout annealing

Annealing time at 300°C	as def.	1h	2h	3.5h
% recrystallised	0	10	25	50
Average band width [μm]	4.2	7.8	7.6	7.1
Nb. of bands investigated	88	67	49	61
Density of bands [mm^{-1}]	36.7	23.9	19.3	15.5
% of bands with $40^\circ\langle 111 \rangle$	19.6	20.9	15.8	9.0

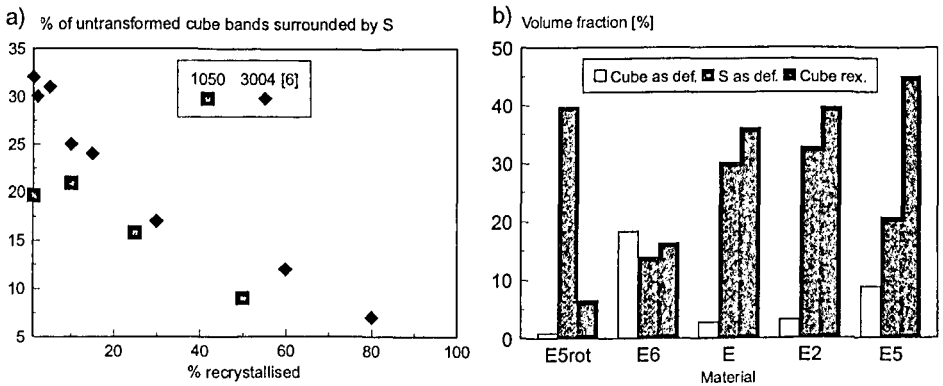


Figure 4. a) fraction of untransformed cube bands with $40^\circ\langle 111 \rangle$ boundary to neighbour, $\epsilon=2$, $Z=10^{14}$, b) fraction of recrystallised cube as a function of amount of S and cube after deformation, $\epsilon=2$, $Z=10^{14}$, [10]

The importance of the S deformation texture component for a strong cube recrystallisation texture is confirmed by the macro texture measurements shown in Fig. 4b), for details see [10]. From this figure, it can be seen that a strong S component in addition to a large fraction of cube bands is necessary to provide a dominating cube texture. A higher level of cube present at the as deformed stage will lead to a higher level of recrystallised cube as long as there is a sufficient amount of S to promote nucleation from the cube bands.

Table 2 gives some additional information on the selective nucleation from cube bands. It can be seen that the average width of untransformed bands after 1h of annealing is considerably larger than in the as deformed condition. This may indicate that nucleation is preferred from the thinnest bands since these have apparently disappeared. This feature is more clearly demonstrated in Fig. 5 which shows the distribution of band widths in the as deformed condition compared to the distribution after 1h of annealing at 300°C . The reason for such a preference may be a higher probability of thin bands being surrounded by high angle boundaries. An alternative explanation for the disappearance is that the thinnest cube bands collapse during the initial annealing stage.

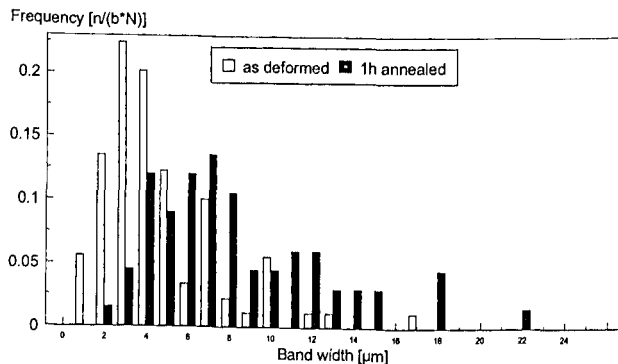


Figure 5. Distribution of cube band widths, as deformed and 1h annealed at 300°C , $\epsilon=2$, $Z=10^{14}$ ($\xi=0.6$, 300°C)

Discussion

The metastability of the cube oriented grains during hot deformation is well documented in Fig. 1. Both the microscopic EBSD-scans measuring line fraction and volume fractions measured by the macroscopic X-ray technique show a decreasing fraction of cube with increasing strain. The effect is enhanced by a higher Zener-Hollomon parameter. Since the measured widths of the cube bands are in accordance with a pure compression mechanism, the decreasing fraction indicates that some cube grains rotate away from the cube position while others remain orientation stable. The observed band widths when applying the high Z value are much smaller than those observed for the lower Z, while the fraction of cube bands is not that much different in the two cases. This must mean that a more heavy deformation, through a high Z value, promotes a splitting up of the original cube grains into layers of thinner cube bands.

The width of all observed cube areas fall into the size that is expected from a compression/smearing out mechanism, with a band width distribution that gets narrower towards smaller values with increasing strain. Further, no signs of transition bands have been found. This means that all cube areas after deformation are due to old cube grains present in the material prior to the deformation. Thus, the idea presented in [6] that old cube grains are smeared out to bands that upon annealing act as nucleation sites for new cube oriented grains, seems to be valid.

The subgrain size measurements might explain why the cube bands are so potent nucleation sites. It turns out that cube subgrains have a size benefit. It can even be stated that some subgrains within cube bands are overcritically large already at the as deformed stage. Such a size advantage has also been demonstrated for a 3004 alloy in Ref. 6 and documented even more extensively by TEM measurements with a very good statistics in Ref. 11. The reason for the large cube subgrains is unclear, but might be due to the orthogonal burgers vectors of the two most active slip systems. This unique cube geometry will facilitate annihilation of active dislocations and thus provide an enhanced recovery rate as proposed by Ridha and Hutchinson [12]. However, what is important in this context is that these large subgrains do exist. While other orientations need annealing to develop successful nuclei, the cube nuclei are already present with overcritical size in the as deformed stage. This, of course, makes cube subgrains very potent nucleation sites and might explain the strong cube recrystallisation texture often found in aluminium.

There seems to be a strong element of a $40^\circ\langle 111 \rangle$ orientation relationship during nucleation and/or growth from the cube bands. The EBSD-results (Fig. 4 and Table 2) clearly indicate that the probability of the nucleation and growth of a cube-oriented recrystallised grain from a cube band is higher when the band is surrounded by the S deformation texture component to which cube makes a $40^\circ\langle 111 \rangle$ boundary. Similar results were also found in Ref. 5 and 6. This S preference is also observed from the macroscopic texture measurements in Fig. 5. It turns out that a large amount of cube prior to deformation is not alone sufficient for a strong recrystallised cube. In addition, a sufficient fraction of S is required for the cube to dominate. The preference of S can be attributed to several reasons. The most obvious is an oriented growth model based on the fact that cube and S make a $40^\circ\langle 111 \rangle$ orientation relationship that is assumed to have a high mobility [9]. This possibility is disputed and was ruled out in [6] since growth rate measurements showed no higher growth rates for cube grains, although the average size of the cube grains was measured to be approximately 15% larger than those of other orientations. This size difference was attributed to other mechanisms, for details see Ref. 6. In the present case grain size measurements in the fully recrystallised condition showed a similar 10% difference

between cube grains and grains of other orientations, i.e. an oriented growth effect cannot be excluded but in line with the conclusions in Ref. 6 seems less likely. This means that the preference is a part of the nucleation stage. It follows from the detailed examination by Vatne et al. [11] that no differences between the stored energy in various deformation texture components were found. This rules out a selectivity mechanism based on a higher amount of stored energy in S. Data on grain boundary energy are insufficient, but a lower energy of the $40^\circ\langle 111 \rangle$ boundary of a high coincidence site density will of course be very important for the nucleation event since the critical Gibbs-Thomson radius is proportional to the boundary energy.

The evolution of the boundary region between two stable neighbour components during deformation, might turn out to be an important aspect. During the EBSP-scans in the present work, these regions have often been observed to be of a random character with subgrains surrounded by low angle boundaries bridging the two components. Such a low angle boundary zone will retard nucleation from the cube band. An interesting speculation now becomes that the transition between a cube grain and an S grain more readily forms a high angle boundary than other components. Such a high angle boundary will be ready to bow out and grow into the matrix. However, much work is required in order to investigate the evolution of boundary areas between stable or metastable deformation texture components. Such a knowledge is necessary in order to be able to explain the selective nucleation from cube bands surrounded by S. In the present work, no experiments have been done to reveal this selectivity. However, the fact that the effect is reproducible in a 1050 alloy is important in itself.

Conclusion

1. Cube oriented grains remain orientation metastable during hot deformation, the degree of stability depending on strain and Zener-Hollomon parameter. During deformation the old cube grains are deformed to band-like shapes which upon annealing act as nucleation sites for cube.
2. Subgrains within the cube bands have a size advantage compared to subgrains of other orientations. This makes the cube bands very potent nucleation sites.
3. The existence of a cube-S high angle boundary promotes nucleation from cube bands.

Acknowledgement: H.E. Vatne and E. Nes want to express their gratitude to the Research Council of Norway and NTH/SINTEF through the "Strong Point Center for Light Metals" for financial support. The partial support to this work from the BRITE/EURAM programme "Microstructural modelling of industrial thermomechanical processing of aluminium alloys" is greatly acknowledged.

References

1. W.G. Burgers and T.J. Tiedema, Acta metal., **1**, 234, (1953)
2. C.S. Barrett, Trans Am. Inst. Min. Engrs., **137**, 128, (1940)
3. I.L. Dillamore, H. Katoh, Met. Sci., **8**, 73, (1994)
4. H. Weiland, J.R. Hirsch, Textures & Microstr., **14-18**, 647, (1991)
5. B.J. Duggan, K. Lücke, G. Köhlhoff, C.S. Lee, Acta metal., **42**, 1921, (1993)
6. H.E. Vatne, O. Daaland, E. Nes, to appear in Proc. of ICOTOM 10, Clausthal, (1993)
7. H.E. Vatne, E. Nes, Scripta metal., **30**, 309, (1994)
8. H.-J. Bunge, Texture Analysis in Materials Science, (Göttingen, Cuvillier Verlag, 1993)
9. B. Liebmam, K. Lücke, G. Masing, Z. Metallkde., **47**, 57, (1956)
10. R.K. Bolingbroke, G. Marshall, R. Ricks, "The Influence of Microstructure on..", these proceedings
11. H.E. Vatne, S. Hofmann, A. Bardal, E. Nes, to be published at ICSMA 10, Sendai, (1994)
12. A.A. Ridha, B.W. Hutchinson, Acta metal., **30**, 1929, (1982)